UNIVERSITY OF CALIFORNIA

Los Angeles

Systemic Delivery of PEGylated NEL-like Molecule-1 (NELL-1) on Ovariectomy-Induced Bone Loss In Mice As a Novel Strategy For Osteoporosis Therapy

A thesis submitted in partial satisfaction

of the requirements for the degree Master of Science

in Oral Biology

by

Chirag Vilas Chawan

2017

ABSTRACT OF THE THESIS

Systemic Delivery of PEGylated NEL-like Molecule-1 (NELL-1) on Ovariectomy-Induced Bone Loss In Mice As a Novel Strategy For Osteoporosis Therapy

by

Chirag Vilas Chawan

Master of Science in Oral Biology

University of California, Los Angeles, 2017

Professor Kang Ting, Chair

Osteoporosis is a metabolic bone disease where decreased bone quality and quantity increases the rate of fractures. It serves as one of the largest skeletal aging problems worldwide. Like many other chronic diseases, osteoporosis affects the majority of the elderly population, especially females after menopause. The prevalence of bone disease and fractures is projected to increase markedly as the population increases(1). Bone disease and many other factors related to fractures will have an enormous impact on the future well-being of Americans and worldwide.

NELL-1 is an osteogenic, secretory molecule previously shown to enhance bone regeneration in various rodent and ovine skeletal defect models. Systemic delivery of NELL-1 via intravenous (IV) injections not only increases murine bone mineral density (BMD) and percent bone volume, but also increases new bone formation throughout the overall skeleton(2). Astoundingly, in the past, we have shown that systemic delivery of NELL-1 induces robust bone formation in healthy mice, which were injected intravenously every 7 days. Here, we investigate the potential of systemic administration of PEGylated NELL-1 (NELL-PEG) every 7 days to see the increases in femoral BMD, percent bone volume and also new bone formation throughout the overall skeleton after four weeks of treatment to reverse ovariectomy (OVX)-induced osteoporotic bone loss in mice. First, we have successfully established osteoporotic mouse model that mimics the human post-menopausal osteoporosis by surgical removal of ovaries. To monitor the changes in BMD *in vivo* dual-energy X-ray absorptiometry (DXA) was performed biweekly. After four weeks of treatment, animals were sacrificed for microCT and histological analyses.

Overall, these findings implied that systemic delivery of NELL-PEG in OVX mice would provide a novel strategy for osteoporosis therapy; nonetheless, further studies are needed to determine the optimum dosage and the efficacy of various routes of drug administration.

Keywords: NELL-1, PEGylation, osteoporosis, systemic osteogenic therapy

The thesis of Chirag Vilas Chawan is approved.

Xinli Zhang

Shen Hu

Carl Maida

Kang Ting, Committee Chair

University of California, Los Angeles

2017

TABLE OF CONTENTS

Abstract.....ii-iii

Introduction

Osteoporosis.....1-2

Current Therapeutics of Osteoporosis.....2-3

NELL-1 and Osteoporosis.....4

PEGylated NELL-1.....5

Materials and Methods

Animals and Surgery 5-6

NELL-PEG intravenous injection.....6

In vivo assessment of BMD by dual-energy X-ray absorptiometry (DXA).....6-7

Ex vivo assessment of bone architecture by microCT.....7-8

Histochemical and immunohistochemical analyses.....8

Statistical Analysis.....9

Results

Confirmation of successful ovariectomy (OVX).....10

In vivo assessment of BMD by dual-energy X-ray absorptiometry (DXA).....10

Ex vivo assessment of bone architecture by microCT.....10-11

Histochemical and immunohistochemical analyses.....11

Discussion.....12-13

Conclusion.....14

Figures and Tables.....15-22

References.....23-26

Acknowledgments

This work was supported partly by NIH/NIAMS grants (R01 AR066782-01, AR068835-01A1, AR061399-01A1), NIH/NIDCR grant (K08DE026805), UCLA/NIH CTSI grant UL1TR000124, and AAOF OFDFA award for J. H. Kwak.

I would like to sincerely thank Drs. Kang Ting, Xinli Zhang, Jin Hee Kwak, Dr. Carl Maida and Dr. Shen Hu for their kind mentoring and guidance, and Drs. Justine Tanjaya, Jiayu Shi, Abdulaziz Mohammad and Hsin Chuan Pan for providing their expertise and proactively supporting many technical aspect of this study.

Lastly, I would like to thank my family, especially my wife Dr. Seemalaxmi Chawan for her continuous support throughout my journey in this project and life.

INTRODUCTION

Osteoporosis

According to the recent report from the World Health Organization, osteoporosis fractures have been one of the heaviest biomedical burdens that far surpassed other noncommunicable diseases(3). Fractures due to osteoporosis are common and place an enormous medical and financial burden on the individual and the nation(4). Alarmingly, stagnation in therapeutics when paired with greater anticipated life-spans and the aging "baby boomer" generation, appears to set up a perfect storm for an even more significant negative impact on the healthcare system. With the increasing aging population nationwide, fracture rates are expected to increase by 48% in the United States alone over the next 25 years, with more than 70% of these cases occurring in postmenopausal women(3, 5). Every year, two million fractures are attributed to osteoporosis, causing more than 432,000 hospital admissions, almost 2.5 million medical office visits, and about 180,000 nursing home admissions in the USA(1). Due in part to an aging population, the cost of care is expected to rise to $25.3 billion by 2025(6). Despite the availability of cost-effective and well-tolerated treatments to reduce fracture risk, only 23% of women more than the age of 67 who have an osteoporosis-related fracture get either a BMD exam or a prescription for a drug to treat osteoporosis within the six months after the fracture(7). Contributing factors such as genetics, advanced age, previous history of fracture, long-term glucocorticoid use, low body weight, menopause, family history of hip fracture, tobacco use, or excess alcohol consumption might contribute to enhanced bone loss. However, the underlying mechanism remains obscure(8). In this

regard, understanding the intercellular regulators that play a significant role in bone metabolism is crucial for planning an effective therapeutic approach for osteoporosis(9, 10). Currently, osteoporosis can be diagnosed before fractures occur with close BMD monitoring by the health professional. There are several effective means of therapeutic intervention to prevent further loss of bone, but none that effectively restores the lost bone at the same time. Thus, the need for dual-functioning anti-resorptive and anabolic therapeutics is real.

Current Therapeutics of Osteoporosis

Current omnipresent therapies for treating osteoporosis are mostly antiresorptive, which inhibits bone resorption and slows down bone turnover. Bisphosphonates, selective estrogen receptor modulators (SERMs), denosumab, estrogen, and calcitonin that are primarily antiresorptive have exhibited remarkable results of treating osteoporosis. However, there are reports that present undesirable side effects such as atypical fractures and osteonecrosis of the jaw(11, 12). Bisphosphonates are considered as first-line therapy for osteoporosis due to its analgesic effects, high efficacy in reducing fractures, and relatively low cost compared with other therapeutic agents(13). However, there are concerns regarding disruption of bone remodeling process and decreased osteoblast activity that may consequently result in diminished bone formation(11, 14). Recent studies regarding monoclonal sclerostin antibody, romosozumab, have shown rapid increases in the spine, hip, and femoral neck BMD based on Phase 2 clinical trials, though there have been reports of hypocalcaemia with severe renal impairments(15-17). Furthermore,

selective cathepsin-K inhibitor, odanacatib, has shown tremendous improvement of BMD, but clinical reports have presented increased risk of atypical fracture(9, 18-23).

On the other hand, teriparatide (PTH 1-34), the only FDA-approved anabolic agent in the U.S. has been shown to not only enhance new bone formation but also improve bone architecture and strength(24, 25). The Randomized clinical trial has shown its efficacy of increasing lumbar and femoral BMD by about 9% and 3%, respectively, on postmenopausal women. Nonetheless, clinical reports revealed that teriparatide could induce hypercalcemia, hypercalciuria, hyperuricemia, and thus it should be prescribed with caution in patients with a history of kidney stones or gout(5, 14).

Despite the substantial advances made in the development of osteoporosis therapeutics, the safety of prolonged use of antiresorptive therapy remains questionable, particularly in the view of increased risk of atypical fracture, cardiovascular health, and side effects in non-targeted craniofacial bones. Currently available anabolic therapies are also indicated for short-term use due to safety concerns. For these reasons, there is an urgent need to develop new dual functioning therapies that are not only effective but also safe.

NELL-1 and Osteoporosis

NELL-1, a novel secretory protein that was first implicated in the context of craniosynostosis, has been shown to increase BMSC numbers, promote osteogenesis, and suppress osteoclastic activity and adipogenesis, without inducing any cytotoxicity (2, 26-30) (Figure 1). This novel osteogenic molecule was highly specific to osteochondral lineage, and recent reports showed that NELL-1 also promotes chondrogenesis in the articular cartilage(31). Prior studies of local delivery of recombinant NELL-1 (rNELL-1) exhibited its potential to reverse osteoporotic bone loss in rodent and ovine models, proving its efficacy as a combined anabolic and anti-osteoclastic agent(2, 31, 32, 36). Interestingly, a genome-wide association study on 2,073 women by Karasik et al. has identified that polymorphism of *NELL-1* is associated with decreased BMD(33). In the osteoporotic rodent model, local delivery of rNELL-1 into the femoral intramedullary cavity significantly enhanced the bone quantity and quality and successfully prevented ovariectomy(OVX)-induced bone loss(41). Furthermore, the efficacy of rNELL-1 to prevent osteoporotic-induced bone loss in mice was demonstrated via systemic, intravenous (IV) administration(36). However, the frequent injection schedule of every other day (q2d) was required due to the short half-life of rNELL-1.

PEGylated-Nell 1

To improve the pharmacokinetics of NELL-1, an FDA-approved method of PEGylation was used(35, 37, 38). NELL-1 protein was covalently conjugated with water-soluble polyethylene glycol (PEG) molecules. Recently, our group has established that PEGylated NELL-1 (NELL-PEG) successfully increases the protein's thermal stability and prolongs the half-life by preserving the osteogenic effects of NELL-1 without any notable cytotoxicity(39). Next, we examined the applicability and safety of NELL-PEG in non-osteoporotic healthy mice, where the weekly systemic administration, through IV tail injection, significantly increased bone mineral density (BMD), trabecular bone formation, and reduced bone resorption in the femur, tibia, and vertebrae. The study successfully demonstrated NELL-PEG's potential as a dual-functioning therapeutic for osteoporosis(2).

The success of previous studies of NELL-1 has led us to the current investigation with the central hypothesis that weekly systemic injection of NELL-PEG could successfully prevent OVX-induced bone loss in mice. This is the first study to test NELL-PEG's efficacy in preventing bone loss in an OVX mouse model.

Materials and Methods:

Animals and Surgery

Three-month-old female C57BL/6 mice were obtained from Charles Rivers Laboratories. Animals were handled under the supervision of the Division of Laboratory Animal Medicine (DLAM) at UCLA in accordance with institutional guidelines of the Chancellor's Animal Research Committee (ARC) of the Office for Protection of Research Subjects.

To generate osteoporosis model that can be used to test the therapeutic effect of NELL-1, animals were divided into two groups: Sham (n=5) and OVX (n=5). Post-operatively, animals underwent biweekly DXA analysis for four weeks to confirm significant bone loss. Then, uteri were harvested, photographed and weighed to confirm atrophy, an indicator of successful OVX.

NELL-PEG intravenous injection

The experimental design and timeline are summarized in Table 1. 15 mice were randomly assigned to Sham-PEG/PBS control, OVX-PEG/PBS control, and OVX-NELL-PEG groups. Animals underwent Sham or OVX operation and biweekly DXA analysis. After confirmation of significant BMD loss in OVX groups at five weeks post-op, animals started receiving therapy via weekly intravenously (IV) injection for four weeks. Animals were anesthetized with isoflurane for the injections. The dosage for NELL-PEG (1.25 mg/kg) was chosen based on our previous study of IV injection in healthy mice(36). The concentration of PEG/PBS (1.52 mg/kg) was calculated to match the total PEG quantity of NELL-PEG.

In vivo assessment of BMD by dual-energy X-ray absorptiometry (DXA)

To monitor dynamic BMD, dual-energy X-ray absorptiometry (DXA) scan was performed biweekly using a Lunar PIXImus II Densitometer (GE Lunar, WI). Under isoflurane anesthesia, all animals were positioned prone on the imaging pad with the femurs parallel to scan direction and knee joints flexed at a right angle. Areal BMD was determined with rectangular regions-of-interest (ROIs) placed on distal femur using image analysis software

(version 2.10) provided by the manufacturer. Data at each time point were generated as relative percent changes in BMD compared to respective pre-treatment values at week 0.

Ex vivo assessment of bone architecture by microCT

Following harvest, femurs and lumbar vertebrae were separated and stored in 4% paraformaldehyde for 48-hours, followed by storage in a 70% ethanol solution. Then, samples were scanned with high-resolution microCT scanner (SkyScan 1172; SkyScan N.V., Belgium), at image resolutions of 27.4 μm (55kV and 181 mA radiation source, using a 0.5-mm aluminum filter). Next, by implementing the Feldkamp algorithm, 2D X-ray projections were used to construct the 3D projections. Appropriate image corrections (including ring artifact correction, beam hardening correction and fine-tuning) were processed via the use of NRecon software (SkyScan N.V., Belgium). The dynamic image range (contrast limits) was determined at 0-0.1 in units of attenuation coefficient and subsequently applied to all datasets for optimal image contrasting.

Following acquisition and reconstruction of all datasets, images were reoriented in each 3D plane using DataViewer software (SkyScan N.V., Belgium). The femurs were aligned along the long axis to be parallel to coronal and sagittal planes. Next, 3D morphometric analysis was performed using CT-Analyzer software (SkyScan N.V., Belgium). The most proximal region of the femoral growth plate as well as the proximal end of the third trochanter were used as reference planes along the long axis, from where femurs were divided into ten equal segments (1 mm = 36 slices). Trabecular regions were defined as the first three distal segments, including the secondary spongiosa in the distal metaphysis. ROIs were

delineated every 5-10 transaxial slices from within the trabecular region, using a freehand drawing tool. Careful consideration was made to separate trabecular structures from endocortical bone by maintaining a 3.5-pixel clearance from the endosteal surface.

A global threshold of 60 (1.01573 g/cm^3) was used to extract a physiologically accurate representation of trabecular bone. Morphometric parameters were then calculated from the binarized images, using direct 3D techniques (marching cubes and sphere-fitting methods). Parameters included bone mineral density (BMD, g/cm^3) and bone volume fraction (BV/TV, %). Each structural and qualitative parameter followed both the nomenclature and units recommended by the American Society for Bone and Mineral Research (ASBMR) Histomorphometry Nomenclature Committee(40) Following data quantification, 3D rendered models were generated for the visualization of analyzed ROI.

Histochemical and immunohistochemical analyses

Femurs were fixed in 4% paraformaldehyde for 24 hours, decalcified in 19% EDTA for 14 days and then embedded in paraffin. Thin sections of 5 microns were prepared and stained with hematoxylin and eosin (H&E), Osteocalcin (OCN) and TRAP staining (Sigma-Aldrich). Immunohistochemistry was carried out using the anti-osteocalcein antibody as a primary antibody and 3-amino-9-ethylcarbazole (AEC) as a chromogen. Olympus BX51 microscope (Olympus Corp.) and cellSens software version 1.6 (Olympus Corp.) were used to view and analyze results. Parameters of osteocalcin+bone-lining cells per bone perimeter (OCN+cells/Bpm, 1/mm) and TRAP+bone-lining cells per bone perimeter (TRAP+cells/Bpm, 1/mm) were used as previously reported(36).

Statistical analysis

Means and standard deviations were calculated for the results. Statistical analysis was performed using Student's t-test was for two group comparisons at 95% confidence levels. Data are presented as mean ± SD, with *P<0.05 and **P<0.01.

Results

Confirmation of successful ovariectomy (OVX)

In the first batch of animals to confirm the successful generation of OVX-induced OVX, uteri were harvested, visually inspected and photographed, and weighed. Figure 2 demonstrates significantly reduced uteri weight and size (Figure 2A) and DXA-measured BMD (Figure 2B) in OVX compared to Sham at four weeks post-op. Successful OVX lead to uterus atrophy and bone loss.

In vivo assessment of BMD by dual-energy X-ray absorptiometry

In the second batch of animals to test therapeutic effect of NELL-PEG in three groups, DXA was performed biweekly *in vivo* for nine weeks (5 weeks of osteoporosis induction plus 4 weeks of treatment). Results were expressed as percent changes in areal BMD relative to the respective pre-treatment values at week 0 of treatment (or 5 weeks post-OVX) (Figure 3). In OVX and Sham PEG/PBS control groups; BMD remained steady at baseline levels in the distal femur throughout the experimental period, while NELL-PEG treatment group exhibited a gradual increase. The discrepancy was statistical significance after four weeks (Sham did not change much from the base line mark and OVX lost 5% from original BMD). Both groups maintained this difference following week four until euthanasia.

Ex vivo assessment of bone architecture by microCT

Ex vivo microCT was used to generate 3D reconstruction of the analyzed femurs (Figure 4) and confirm DXA findings of reduced bone density. Trabecular bone formation was increased in OVX-NELL-PEG group compared to OVX-PEG/PBS (Figure 4). Femoral BMD

and BV/TV were increased in OVX-NELL-PEG animals compared to OVX-PEG/PBS control (Figure 5).

Histological and immunohistochemical analyses

H&E stain showed reduced femoral trabecular formation in OVX control compared to OVX NELL-PEG group (Figure 6). Immunohistochemistry showed reduced TRAP-positive cells (osteoclasts) and increased OCN expression in OVX NELL-PEG group compared to OVX PEG/PBS control, indicative of NELL-PEG's anti-resorptive and pro-osteogenic properties (Figure 6).

Discussion

In this study, we performed OVX surgery on mice to mimic osteoporosis-induced bone loss in humans. The effectiveness of OVX was confirmed by significant uterine atrophy and decreased BMD as measured by DXA analysis four weeks post-surgery (Figure 2). The lumbar BMD was significantly reduced by 8.6% compared to the Sham. After successfully testing induction of bone loss with the first batch of animals, we proceeded to examine the therapeutic effects of NELL-PEG with the second batch of animals in three groups: 1) Sham-PEG/PBS control, 2) OVX-PEG/PBS control, and 3) OVX-NELL-PEG. After five weeks of osteoporosis induction, NELL-PEG or PEG/PBS control were injected intravenously on a weekly basis for four weeks (Table 1). Throughout the study period, DXA scans were performed biweekly to monitor changes in BMD. Excitingly, we found that the OVX-NELL-PEG group demonstrated significantly increased BMD after weekly NELL-PEG injection compared to baseline by the second week (Figure 3). After four weeks of NELL-PEG administration, the BMD of the OVX-NELL-PEG group was significantly higher than that of the OVX and Sham control groups, which largely remained constant throughout treatment (Figure 3). Consistent with the DXA data, immunohistochemistry staining with OCN and TRAP exhibited increased osteoblastic activity and decreased osteoclastic activity at the distal femoral metaphysis (Figure 6). This result is consistent with our previous findings that NELL-1 has a dual anabolic and anti-resorptive effect that can serve as a novel therapy for the treatment of osteoporosis(2, 36, 41).

In contrast, microCT measurements revealed that although the BMD of the OVX-NELL-PEG group was higher than that of the OVX-PEG/PBS group with low significance, the percent bone volume (BV/TV) values were comparable (Figure 5). One possible explanation for this result may be attributed to our study limitations. Specifically, our study had a modest sample size and a relatively low dose, as the dosage of 1.25mg/kg of NELL-PEG was determined based on previous injection studies in healthy mice. In addition, studies have shown that OVX-induced bone loss varies among inbred strains of mice, and that C57BL/6 mice may not be the best strain to detect changes in the trabecular bone. This is due to the fact that C57BL/6 mice inherently have reduced trabecular bone volume compared to other strains such as BALB/c mice(10). Furthermore, long-term studies of IV-delivered systemic drugs may induce irritation to the veins. Consequently, it is crucial to explore alternative routes of systemic administration, which may improve safety and ease of manipulation without diminishing the efficacy of the drug(42). Overall, the results indicate that weekly intravenous administration of NELL-PEG can reverse osteoporotic bone loss in mice, although not definitively. Future studies are needed not only to optimize the dosing, but also to refine the bone-targeting efficiency of NELL-PEG to achieve definitive success in reversing OVX-induced osteoporosis in mice. Nevertheless, NELL-PEG holds great potential as a novel therapy for the treatment of osteoporosis.

Conclusion

In conclusion, the results of this study showed that systemic delivery of NELL-PEG in OVX mice via intravenous injection results in significantly increased bone mineral density, increased osteoblastic activity, and decreased osteoclastic activity compared to the PEG/PBS control. Although the microCT results showed that weekly IV administration of NELL-PEG did not significantly increase percent bone volume, this study provided solid rationale to continue developing NELL-PEG as a systemic therapy for the treatment of osteoporosis. Future studies incorporating a larger sample size, longer treatment durations, varying dosages, and alternative routes of administration are necessary to further optimize NELL-PEG as a viable osteoporosis therapy. Looking ahead, NELL-PEG holds tremendous potential as a powerful anti-osteoporotic therapy that can significantly improve patient outcomes and quality of life with profound clinical implications.

FIGURES AND TABLES

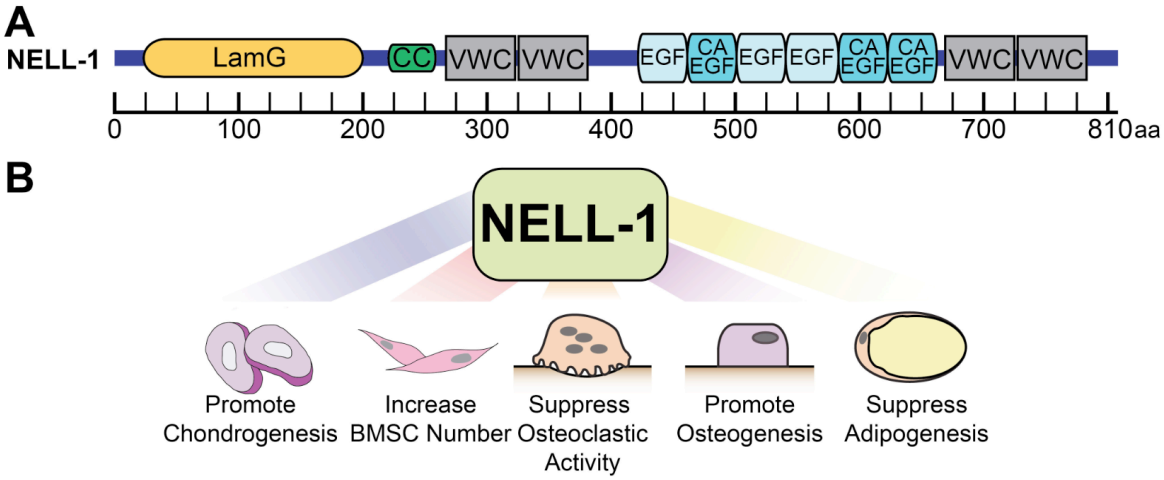

Figure 1. NELL-1 structure and function. (A) Distinct domains within the structure of NELL-1 include LamG: Laminin G domain, VWC: Von Willebrand type C domain, CC: Coiled-coil regions, CA EGF: Calcium binding EGF-like domains. (B) Known functions of NELL-1 to date. The current proposal will focus on osteoblastogenic and anti-osteoclastic effects of NELL-1 (26, 36).

A

	Operation	Sample size	Treatment
Batch 1	Sham	5	-
	OVX	5	-
Batch 2	Sham	5	PEG/PBS (1.52mg/kg)
	OVX	5	PEG/PBS (1.52mg/kg)
	OVX	5	NELL-PEG (1.25mg/kg)

B

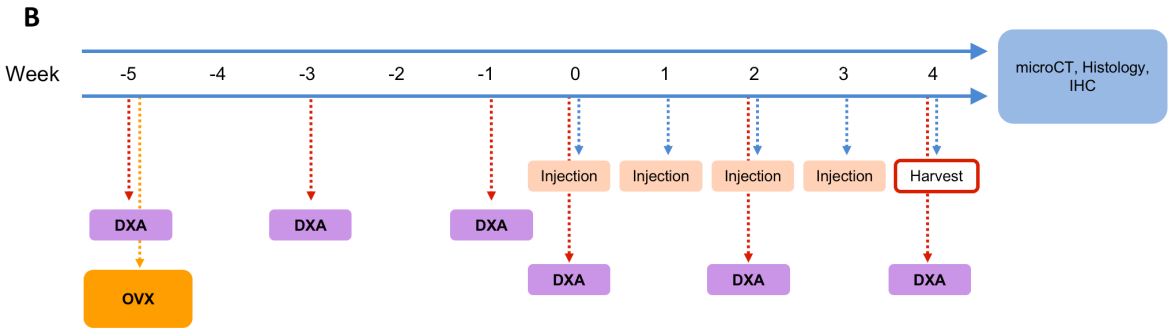

Table 1. Experimental Design. (A) Animal grouping for Batch 1 and Batch 2 (n=5/group). (B) Timeline and procedures for Batch 2.

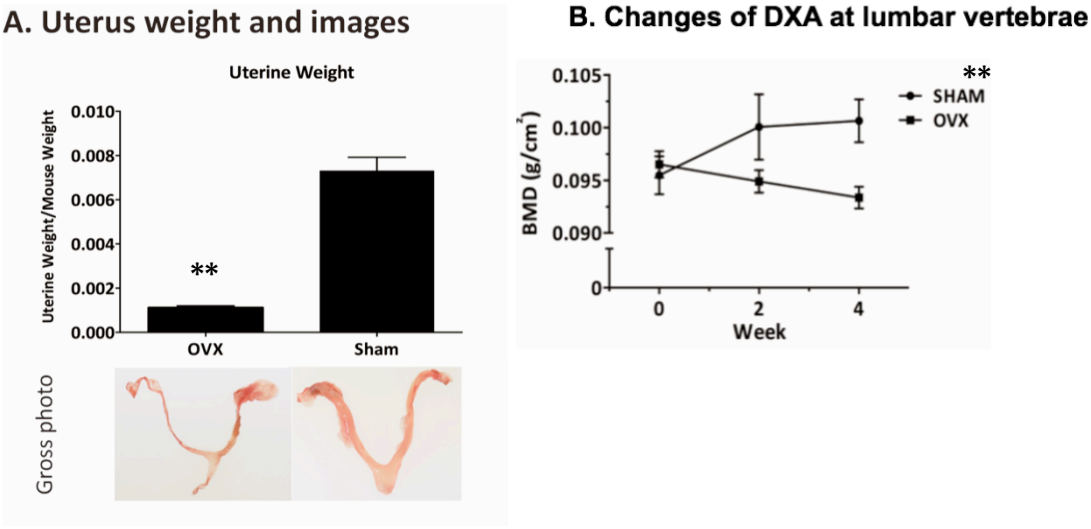

FIGURE 2. Confirmation of successful OVX and bone loss by visual inspection, photography, weight, and DXA analyses. (a) OVX shows significantly reduced uteri weight (top) and size (bottom) compared to Sham. (B) DXA analysis showed significant BMD decrease in OVX at 4 weeks post-op.

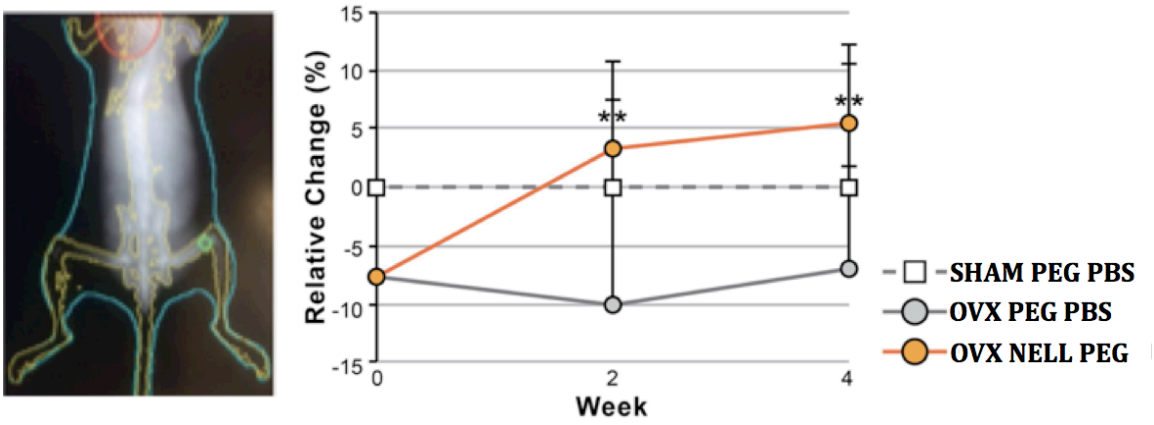

FIGURE 3. ***In vivo*** **assessment of BMD by DXA.** To monitor the changing BMD in the femurs of systemically treated mice, DXA was performed biweekly. Results were expressed as percent changes in areal BMD relative to the respective pre-treatment values at week 0 of treatment (or at 5 weeks post-OVX). NELL-PEG group showed gradual and significant increases in BMD compared to the cognate vehicle controls.

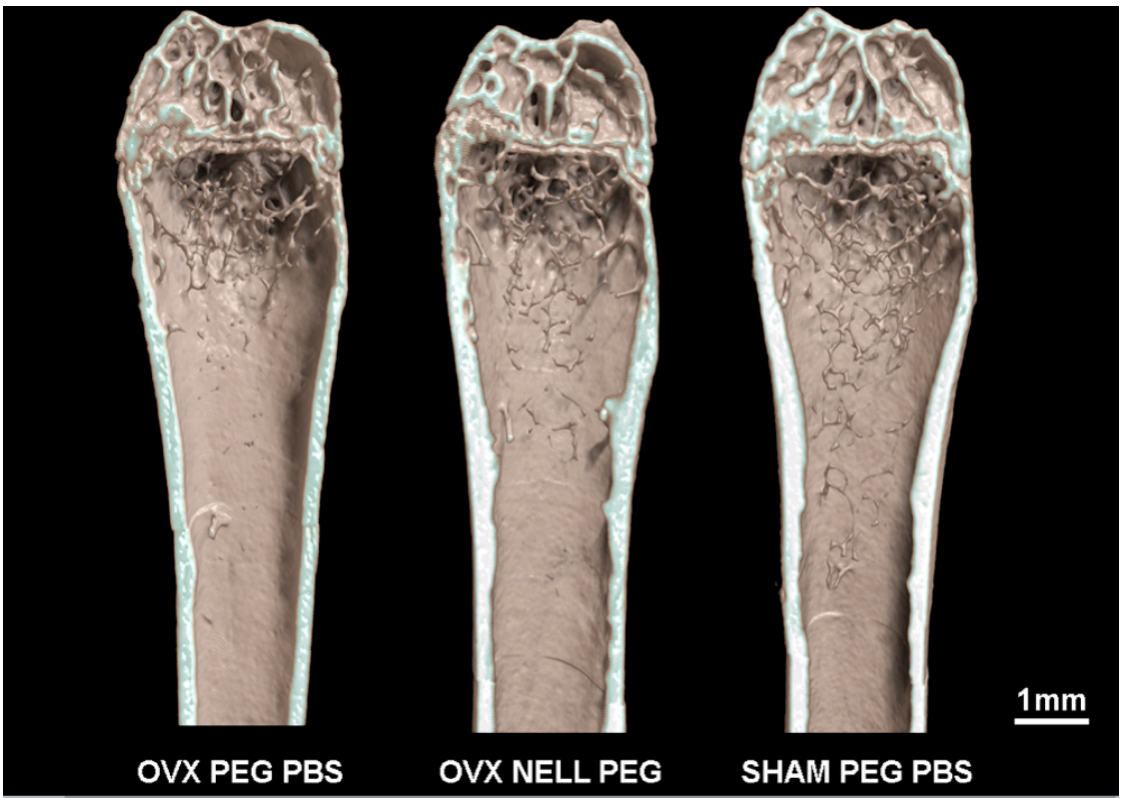

OVX: NELL-PEG OVX: PEG/PBS

FIGURE 4. Ex vivo assessment of bone architecture by microCT. 3D reconstruction of the distal half of the femurs are shown to demonstrate significantly increased trabecular bones that longitudinally filled more of the marrow space in OVX-NELL-PEG group compared to OVX-PEG/PBS control. The amount of the bone is comparable to Sham control.

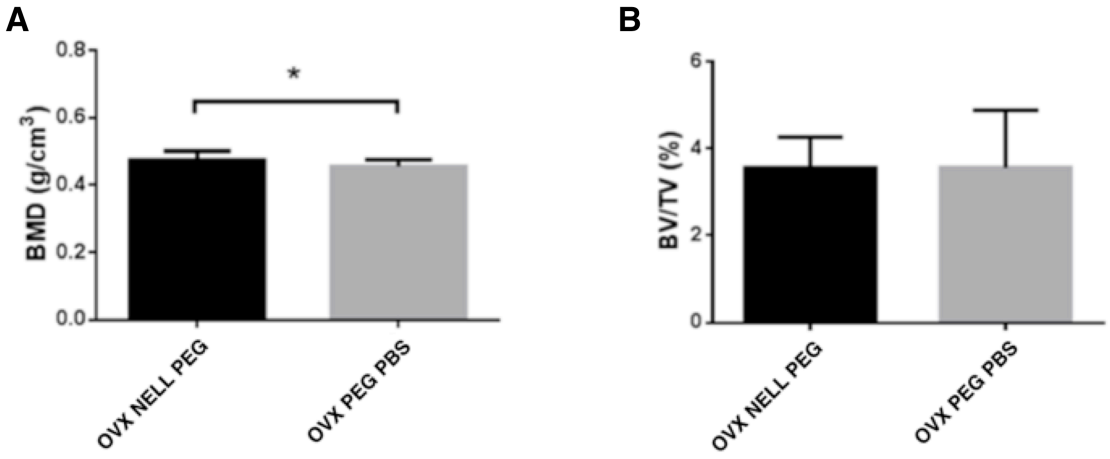

FIGURE 5. MicroCT quantification of OVX NELL-PEG and PEG/PBS femoral trabecular bones. Although BMD quantification shows significant increase in NELL-PEG group compared to PEG/PBS control (A), BV/TV quantification did not show significance (B).

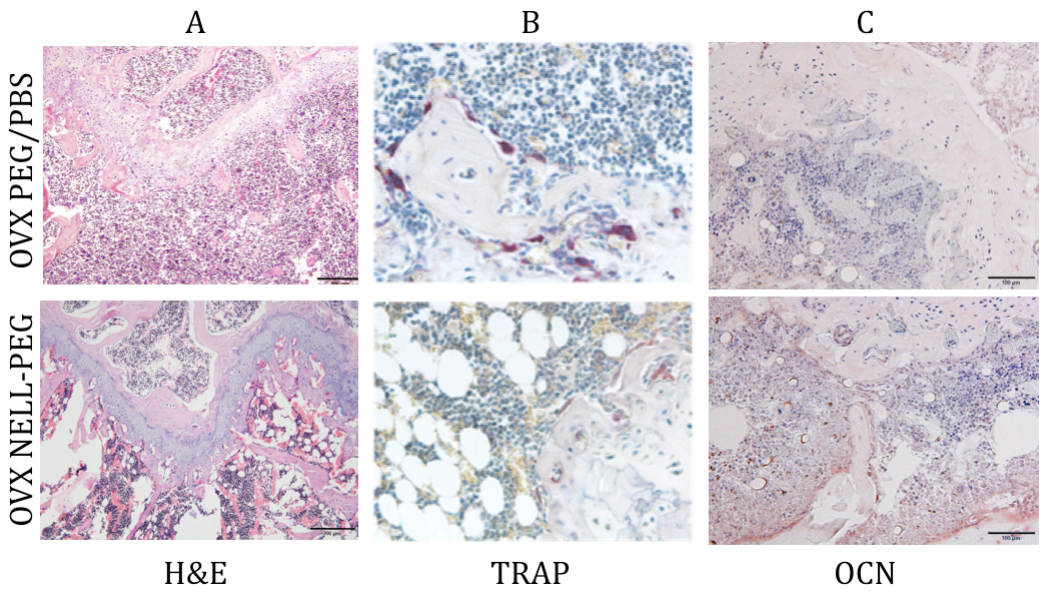

FIGURE 6. Histological and Immunohistochemical Analyses. (A) H&E staining exhibited greater trabecular bone formation at the distal femoral metaphysis in the NELL-PEG group compared to PEG/PBS control. (B) TRAP staining exhibited a reduction in TRAP positive-cells in the NELL-PEG treated femurs compared to control. (C) The number of osteocalcin (OCN) positive-cells were increased in NELL-PEG femurs compared to control.

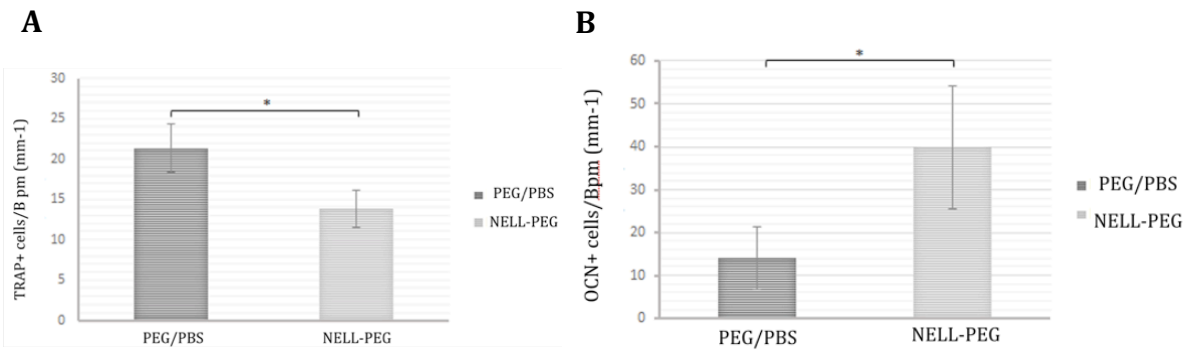

FIGURE 7. Quantification of Immunohistochemical staining. NELL-PEG group exhibited significantly reduced TRAP positive-cells (A) and significantly increased OCN-positive cells (B) compared to PEG/PBS control, indicative of a dual anti-osteoclastic and pro-osteoblastic property of NELL-PEG.

REFERENCES

1. Bone Health and Osteoporosis: A Report of the Surgeon General. Rockville (MD)2004.

2. Kwak, J.H., Zhang, Y., Park, J., Chen, E., Shen, J., Chawan, C., Tanjaya, J., Lee, S., Zhang, X., Wu, B.M., Ting, K., andSoo, C. Pharmacokinetics and osteogenic potential of PEGylated NELL-1 in vivo after systemic administration. Biomaterials **57**, 73, 2015.

3. Sheu, Y., Amati, F., Schwartz, A.V., Danielson, M.E., Li, X., Boudreau, R., Cauley, J.A., andOsteoporotic Fractures in Men Research, G. Vertebral bone marrow fat, bone mineral density and diabetes: The Osteoporotic Fractures in Men (MrOS) study. Bone **97**, 299, 2017.

4. Cosman, F., de Beur, S.J., LeBoff, M.S., Lewiecki, E.M., Tanner, B., Randall, S., Lindsay, R., andNational Osteoporosis, F. Clinician's Guide to Prevention and Treatment of Osteoporosis. Osteoporos Int **25**, 2359, 2014.

5. O'Connor, K.M. Evaluation and Treatment of Osteoporosis. Med Clin North Am **100**, 807, 2016.

6. Burge, R., Dawson-Hughes, B., Solomon, D.H., Wong, J.B., King, A., andTosteson, A. Incidence and economic burden of osteoporosis-related fractures in the United States, 2005-2025. J Bone Miner Res **22**, 465, 2007.

7. Cosman, F., de Beur, S.J., LeBoff, M.S., Lewiecki, E.M., Tanner, B., Randall, S., andLindsay, R. Erratum to: Clinician's guide to prevention and treatment of osteoporosis. Osteoporos Int **26**, 2045, 2015.

8. Wang, C., Shan, S., Wang, C., Wang, J., Li, J., Hu, G., Dai, K., Li, Q., andZhang, X. Mechanical stimulation promote the osteogenic differentiation of bone marrow stromal cells through epigenetic regulation of Sonic Hedgehog. Exp Cell Res 2017.

9. Tabatabaei-Malazy, O., Salari, P., Khashayar, P., andLarijani, B. New horizons in treatment of osteoporosis. Daru **25**, 2, 2017.

10. Bouxsein, M.L., Myers, K.S., Shultz, K.L., Donahue, L.R., Rosen, C.J., andBeamer, W.G. Ovariectomy-induced bone loss varies among inbred strains of mice. J Bone Miner Res **20**, 1085, 2005.

11. James, A.W., LaChaud, G., Shen, J., Asatrian, G., Nguyen, V., Zhang, X., Ting, K., andSoo, C. A Review of the Clinical Side Effects of Bone Morphogenetic Protein-2. Tissue Eng Part B Rev **22**, 284, 2016.

12. Shen, J., James, A.W., Zara, J.N., Asatrian, G., Khadarian, K., Zhang, J.B., Ho, S., Kim, H.J., Ting, K., andSoo, C. BMP2-Induced Inflammation Can Be Suppressed by the Osteoinductive Growth Factor NELL-1. Tissue Engineering Part A **19**, 2390, 2013.

13. Ishtiaq, S., Fogelman, I., andHampson, G. Treatment of post-menopausal osteoporosis: beyond bisphosphonates. J Endocrinol Invest **38**, 13, 2015.

14. Lopez-Delgado, L., Riancho-Zarrabeitia, L., andRiancho, J.A. Genetic and acquired factors influencing the effectiveness and toxicity of drug therapy in osteoporosis. Expert Opin Drug Metab Toxicol **12**, 389, 2016.

15. Kalem, M.N., Kalem, Z., Akgun, N., andBakirarar, B. The relationship between postmenopausal women's sclerostin levels and their bone density, age, body mass index, hormonal status, and smoking and consumption of coffee and dairy products. Arch Gynecol Obstet **295**, 785, 2017.

16. Bandeira, L., Lewiecki, E.M., andBilezikian, J.P. Romosozumab for the treatment of osteoporosis. Expert Opin Biol Ther **17**, 255, 2017.

17. Ma, Y.L., Hamang, M., Lucchesi, J., Bivi, N., Zeng, Q., Adrian, M.D., Raines, S.E., Li, J., Kuhstoss, S.A., Obungu, V., Bryant, H.U., andKrishnan, V. Time course of disassociation of bone formation signals with bone mass and bone strength in sclerostin antibody treated ovariectomized rats. Bone **97**, 20, 2016.

18. Duong, L.T., Crawford, R., Scott, K., Winkelmann, C.T., Wu, G., Szczerba, P., andGentile, M.A. Odanacatib, effects of 16-month treatment and discontinuation of therapy on bone mass, turnover and strength in the ovariectomized rabbit model of osteopenia. Bone **93**, 86, 2016.

19. Vermeire, J.J., Suzuki, B.M., andCaffrey, C.R. Odanacatib, a Cathepsin K Cysteine Protease Inhibitor, Kills Hookworm In Vivo. Pharmaceuticals (Basel) **9**2016.

20. Garber, K. Two pioneering osteoporosis drugs finally approach approval. Nat Rev Drug Discov **15**, 445, 2016.

21. Duong, L.T., Pickarski, M., Cusick, T., Chen, C.M., Zhuo, Y., Scott, K., Samadfam, R., Smith, S.Y., andPennypacker, B.L. Effects of long term treatment with high doses of odanacatib on bone mass, bone strength, and remodeling/modeling in newly ovariectomized monkeys. Bone **88**, 113, 2016.

22. Gennari, L., Rotatori, S., Bianciardi, S., Nuti, R., andMerlotti, D. Treatment needs and current options for postmenopausal osteoporosis. Expert Opin Pharmacother **17**, 1141, 2016.

23. Chapurlat, R. Cathepsin K inhibitors and antisclerostin antibodies. The next treatments for osteoporosis? Joint Bone Spine **83**, 254, 2016.

24. Dempster, D.W., Zhou, H., Recker, R.R., Brown, J.P., Recknor, C.P., Lewiecki, E.M., Miller, P.D., Rao, S.D., Kendler, D.L., Lindsay, R., Krege, J.H., Alam, J., Taylor, K.A., Janos, B., andRuff, V.A. Differential Effects of Teriparatide and Denosumab on Intact PTH and Bone Formation Indices: AVA Osteoporosis Study. J Clin Endocrinol Metab **101**, 1353, 2016.

25. Miyauchi, A. [Relationship of pharmacokinetics, changes of bone turnover markers and BMD/fractures efficacy during treatment with anabolic agents;Teriparatide daily and once weekly subcutaneous injections.]. Clin Calcium **26**, 1583, 2016.

26. Zhang, X., Zara, J., Siu, R.K., Ting, K., andSoo, C. The role of NELL-1, a growth factor associated with craniosynostosis, in promoting bone regeneration. J Dent Res **89**, 865, 2010.

27. Aghaloo, T., Jiang, X., Soo, C., Zhang, Z., Zhang, X., Hu, J., Pan, H., Hsu, T., Wu, B., Ting, K., andZhang, X. A study of the role of nell-1 gene modified goat bone marrow stromal cells in promoting new bone formation. Mol Ther **15**, 1872, 2007.

28. Aghaloo, T., Cowan, C.M., Chou, Y.F., Zhang, X., Lee, H., Miao, S., Hong, N., Kuroda, S., Wu, B., Ting, K., andSoo, C. Nell-1-induced bone regeneration in calvarial defects. Am J Pathol **169**, 903, 2006.

29. Zhang, X., Cowan, C.M., Jiang, X., Soo, C., Miao, S., Carpenter, D., Wu, B., Kuroda, S., andTing, K. Nell-1 induces acrania-like cranioskeletal deformities during mouse embryonic development. Lab Invest **86**, 633, 2006.

30. Zhang, X., Carpenter, D., Bokui, N., Soo, C., Miao, S., Truong, T., Wu, B., Chen, I., Vastardis, H., Tanizawa, K., Kuroda, S., andTing, K. Overexpression of Nell-1, a craniosynostosis-associated gene, induces apoptosis in osteoblasts during craniofacial development. J Bone Miner Res **18**, 2126, 2003.

31. Li, C.S., Zhang, X., Peault, B., Jiang, J., Ting, K., Soo, C., andZhou, Y.H. Accelerated Chondrogenic Differentiation of Human Perivascular Stem Cells with NELL-1. Tissue Eng Part A **22**, 272, 2016.

32. James, A.W., Chiang, M., Asatrian, G., Shen, J., Goyal, R., Chung, C.G., Chang, L., Shrestha, S., Turner, A.S., Seim, H.B., 3rd, Zhang, X., Wu, B.M., Ting, K., andSoo, C. Vertebral Implantation of NELL-1 Enhances Bone Formation in an Osteoporotic Sheep Model. Tissue Eng Part A **22**, 840, 2016.

33. Karasik, D., Hsu, Y.H., Zhou, Y., Cupples, L.A., Kiel, D.P., andDemissie, S. Genome-wide pleiotropy of osteoporosis-related phenotypes: the Framingham Study. J Bone Miner Res **25**, 1555, 2010.

34. Lee, S., Zhang, X., Shen, J., James, A.W., Chung, C.G., Hardy, R., Li, C., Girgius, C., Zhang, Y., Stoker, D., Wang, H., Wu, B.M., Peault, B., Ting, K., andSoo, C. Brief Report: Human

Perivascular Stem Cells and Nel-Like Protein-1 Synergistically Enhance Spinal Fusion in Osteoporotic Rats. Stem Cells **33**, 3158, 2015.

35. Batra, J., Robinson, J., Mehner, C., Hockla, A., Miller, E., Radisky, D.C., andRadisky, E.S. PEGylation extends circulation half-life while preserving in vitro and in vivo activity of tissue inhibitor of metalloproteinases-1 (TIMP-1). PLoS One **7**, e50028, 2012.

36. James, A.W., Shen, J., Zhang, X., Asatrian, G., Goyal, R., Kwak, J.H., Jiang, L., Bengs, B., Culiat, C.T., Turner, A.S., Seim Iii, H.B., Wu, B.M., Lyons, K., Adams, J.S., Ting, K., andSoo, C. NELL-1 in the treatment of osteoporotic bone loss. Nat Commun **6**, 7362, 2015.

37. Dozier, J.K., andDistefano, M.D. Site-Specific PEGylation of Therapeutic Proteins. Int J Mol Sci **16**, 25831, 2015.

38. Huang, Z., Zhu, G., Sun, C., Zhang, J., Zhang, Y., Zhang, Y., Ye, C., Wang, X., Ilghari, D., andLi, X. A novel solid-phase site-specific PEGylation enhances the in vitro and in vivo biostabilty of recombinant human keratinocyte growth factor 1. PLoS One **7**, e36423, 2012.

39. Zhang, Y., Velasco, O., Zhang, X., Ting, K., Soo, C., andWu, B.M. Bioactivity and circulation time of PEGylated NELL-1 in mice and the potential for osteoporosis therapy. Biomaterials **35**, 6614, 2014.

40. Parfitt, A.M. Bone histomorphometry: proposed system for standardization of nomenclature, symbols, and units. Calcif Tissue Int **42**, 284, 1988.

41. Kwak, J., Zara, J.N., Chiang, M., Ngo, R., Shen, J., James, A.W., Le, K.M., Moon, C., Zhang, X., Gou, Z., Ting, K., andSoo, C. NELL-1 Injection Maintains Long-Bone Quantity and Quality in an Ovariectomy-Induced Osteoporotic Senile Rat Model. Tissue Engineering Part A **19**, 426, 2013.

42. Tanjaya, J., Zhang, Y., Lee, S., Shi, J., Chen, E., Ang, P., Zhang, X., Tetradis, S., Ting, K., Wu, B., Soo, C., andKwak, J.H. Efficacy of Intraperitoneal Administration of PEGylated NELL-1 for Bone Formation. Biores Open Access **5**, 159, 2016.